Antarctic krill oil high internal phase Pickering emulsion stabilized by bamboo protein gels and the anti-inflammatory effect in vitro and in vivo

Minghao Zhang, Jinrui Zhu, Li Zhou, Jianquan Kan, Minjie Zhao, Rong Huang, Jikai Liu, Eric Marchioni

Journal of Functional Foods 94 (2022) 105134

Contents lists available at ScienceDirect

Journal of Functional Foods

journal homepage: www.elsevier.com/locate/jff

Antarctic krill oil high internal phase Pickering emulsion stabilized by bamboo protein gels and the anti-inflammatory effect *in vitro* and *in vivo*

Minghao Zhang [a], Jinrui Zhu [a], Li Zhou [a,*], Jianquan Kan [b,*], Minjie Zhao [c], Rong Huang [a], Jikai Liu [a,*], Eric Marchioni [c]

[a] National Demonstration Center for Experimental Ethnopharmacology Education, School of Pharmaceutical Sciences, South-Central MinZu University, Wuhan 430074, PR China

[b] College of Food Science, Southwest University, Chongqing 400715, PR China

[c] Inst Pluridisciplinaire Hubert Curien, CNRS, Equipe Chim Analyt Mol Bioact & Pharmacognoise, UMR 7178, UDS, F-67400 Illkirch Graffenstaden, France

ARTICLE INFO

Keywords:
Fungus
Delivery system
Preparation
Pickering stabilizer
Anti-inflammatory
Ulcerative colitis

ABSTRACT

This study aims to introduce a high internal phase Pickering emulsion (HIPPE) stabilized by bamboo fungus protein gel particles (BGPs), incorporating Antarctic krill oil (KO), as a new delivery formulation to enrich the application of KO. The appropriate proportion of KO (2:8) contributed to HIPPE stabilization (φ = 80%). At pH 11, strong electrostatic interaction tended to produce KO-HIPPE with small droplet and homogeneous size (1.5 μm). BGPs dosage either under (0.5%) or high (2.0%) was prone to the destabilization of KO-HIPPE. *In vitro* studies indicated that KO-HIPPE had no effect on cell viability and suggested the safety and anti-inflammatory effect. *In vivo* studies showed that KO-HIPPE treatment could improve the clinical symptoms, suppress the overexpression of the pro-inflammatory cytokines (TNF-α and IL-6) and protect the intestinal barrier with function. The findings demonstrated that the HIPPE stabilized on BGPs had excellent loading efficiency of KO and good security, stability and functional activity.

1. Introduction

High internal phase Pickering emulsion (HIPPE) are emulsions stabilized by solid particles with an internal phase volume fraction (φ) exceeding 74%. Solid particles with proper particle size, wettability and surface charge were irreversibly adsorbed at the phase interface to constitute stable HIPPE, which could resist flocculation and Ostwald ripening, provide unique storage stability and environmental stability. Different from the fluid state of traditional emulsions, in HIPPE, droplets were tightly packed together to form a semi-solid material with viscoelasticity (Wen, Zhang, Jin, Sui, & Jiang, 2020), which could be used as a mayonnaise substitute to reduce trans fatty acid intake due to its similar rheological behavior and texture (Liu et al., 2018). HIPPE as a porous material template has demonstrated to be one of the most effective techniques for generating pore structures. In addition, HIPPE are oil–water two-phase systems that have the same function as emulsions to encapsulate and deliver nutrients (Santos, Okuro, & Cunha, 2021). HIPPE have attracted high attention due to the wide source of materials, simple preparation process, outstanding stability and multiple functional properties.

New solid particle stabilizers have been discovered, including various inorganic or organic particles, synthetic materials, etc. (Jafari, Doost, Nasrabadi, Boostani, & Van der Meeren, 2020; Sharkawy, Barreiro, & Rodrigues, 2020). Due to the green environmental concept, HIPPE stabilizer with biomolecule protein is main direction of research. Proteins obtained from soy, peanut, corn and wheat are commonly used as plant proteins (Huang et al., 2019). Soy and peanut protein gel particles (1.5 wt%) could stabilize HIPPE with 82% and 88% of phase volume fraction, respectively (Jiao, Shi, Wang, & Binks, 2018; Wen et al., 2020). Marketed animal proteins such as whey protein, ovalbumin, and bovine serum protein were also suitable raw materials for HIPPE stabilizers (Huang et al., 2019). In comparison, fungus, as

Abbreviations: HIPPE, high internal phase Pickering emulsion; BGPs, bamboo fungus protein gel particles; KO, Antarctic krill oil; KO-HIPPE, Antarctic krill oil high internal phase Pickering emulsion; DSS, Dextran sulfate sodium; PUFAs, polyunsaturated fatty acids; EPA, eicosapentaenoic acid; DHA, docosahexaenoic acid; PLs, phospholipids; FFA, free fatty acids; FBS, fetal bovine serum; LPS, Lipopolysaccharide; CLSM, confocal laser scanning microscopy; SSF, simulated saliva fluid; SGF, simulated gastric fluid; SIF, simulated intestinal fluid; UC, ulcerative colitis; DAI, calculation of disease activity index; H&E, hematoxylin and eosin.

* Corresponding authors.
E-mail addresses: zhou2018@scuec.edu.cn (L. Zhou), ganjq1965@163.com (J. Kan), 2380471675@qq.com (J. Liu).

https://doi.org/10.1016/j.jff.2022.105134
Received 26 February 2022; Received in revised form 11 May 2022; Accepted 23 May 2022

another broad source of proteins, has been underappreciated for its great potential in HIPPE stabilizer. Our previous study has established HIPPE based on bamboo fungus protein gel particles (BGPs), and its microstructure and stabilization mechanism were investigated (Zhang et al., 2021). Here, the functional properties and applications were discussed in this study.

Based on the characteristics of good biocompatibility and high oil loading capacity, HIPPE stabilized by protein particles have promising applications in food and pharmaceutical fields as substance encapsulation and delivery systems (Santos et al., 2021). Pickering emulsions composed of zein particles with cinnamon essential oil can replace 20% of butter, reducing fat intake and inhibiting microbial growth to extend shelf life (Feng et al., 2020). Pickering formulations with chitosan/collagen peptide nanoparticles were suitable as a topical delivery vehicle (Sharkawy, Barreiro, & Rodrigues, 2021; Sharkawy, Silva, Rodrigues, Barreiro, & Rodrigues, 2021). Fish oil which contained high levels of polyunsaturated fatty acids (PUFAs), especially n-3 eicosapentaenoic acid (EPA; C20:5) and docosahexaenoic acid (DHA; C22:6), in the presence of tea protein/carrageenan complex particles forming stable o/w Pickering emulsions, thus could expand the application of fish oil (Ren et al., 2021).

Antarctic krill oil (KO), obtained from *Euphausia superba*, is a marine functional oil that enriched with long-chain omega-3 PUFAs, especially EPA and DHA (Zhou et al., 2021a). Compared to fish oil, the n-3 PUFAs in KO is mainly bound with phospholipids (PLs) rather than triglycerides (TAG) so that the bioavailability of n-3 PUFAs was higher in KO form (Liu et al., 2014). Dietary intake of KO for one month has been demonstrated to protect oxidative stress, neuroinflammation and cognitive impairment (Choi et al., 2017). In addition to the low solubility and oxidative instability of KO, the presence of unpleasant odor and taste results in unacceptable to consumers. Therefore, further refinement of its delivery system is necessary to provide the same health benefits at an attractive dosage and intake formulation. Distinguishing from existing KO microcapsules and conventional o/w emulsions (Sánchez, Zavaleta, García, Solano, & Díaz, 2021), HIPPE encapsulated with KO is a new attempt. On the one hand, HIPPE can modify the solubility of oil and provide protection against UV light, heat, and oxidation (Sharkawy, Casimiro, Barreiro, & Rodrigues, 2020; Zhou et al., 2018). On the other hand, HIPPE can alter the extent and rate of lipolysis of oil after gastrointestinal digestion, accelerating or decreasing the release of free fatty acids (FFA) depending on their interfacial composition and properties (Yi, Gao, Zhong, & Fan, 2020). Finally, in combination with HIPPE system, a new health food containing KO could be formulated to expand the KO applications.

In present study, KO was delivered via BGPs stabilized HIPPE. Firstly, the preparation conditions of KO-HIPPE were investigated, and their structure and stability were evaluated. Then, the immunostimulatory activity of KO-HIPPE were determined by *in vitro* and *in vivo* experiments.

2. Reagents and materials

2.1. Materials

Dried bamboo fungi (*Dictyophora indusiata*) were purchased from Yunnan wild fungus Market. Transglutaminase (120 U/g), mucin type II, pepsin (>3000 U/mg), lipase (20000 U/g), pancreatin (130 U/mg), bile salt (from pig), and soybean oil were purchased from Macklin Biochemical Technology (Shanghai, China). Analytical grade NaOH, HCl, NaCl, $CaCl_2$ and PBS buffer were also purchased from Macklin Biochemical Technology. Antarctic krill oil obtained from Qingdao Kangjing Marine Biotechnology Co., Ltd (Shandong, China). DMEM medium and fetal bovine serum (FBS) were obtained from HyClone (Logan, USA) and Tianhang Biochemical Technology (Hangzhou, China), respectively. Lipopolysaccharide (LPS, *Escherichia coli*) and dextran sulfate sodium salt (DSS, MW: 40,000) were obtained from Aladdin Biochemical Technology (Shanghai, China). GAPDH Rabbit mAb, occludin Rabbit pAb, and HRP Goat Anti-Rabbit IgG (H + L) were purchased from ABclonal Technology (Wuhan, China). The ELISA kits of IL-6 and TNF-α were purchased from Xinbosheng Biotechnology (Shenzhen, China). Methylthiazolyldiphenyl-tetrazolium bromide (MTT), 4% Paraformaldehyde fix solution, physiological saline solution, RIPA Lysis Buffe, and bicinchoninic acid (BCA) protein concentration assay kits were obtained from Beyonte Biotechnology (Shanghai, China). Urine fecal occult blood test kit, SOD, MDA and GSH kits were purchased from Nanjing Jiancheng Institute of Biological Engineering (Nanjing, China).

2.2. Animals and cell

Male C57BL/6 mice (18–22 g, 4–5 weeks) were purchased from Liaoning Changsheng biotechnology (Certificate SCXK2020-0001; Shenyang, China). All mice were maintained under standard specific pathogen-free conditions with a 12 h light/dark cycle for 1 week. Animal use and care were confirmed by the Animal Experimental Ethics Committee of South-Central University for Nationalities (SYXK, Wuhan 2016–0089, No. 2019-SCUEC-AEC-014).

RAW 264.7 cells purchased from China Center for Type Culture Collection (CCTCC, Wuhan, China) were cultured in Dulbecco's modification of Eagle's medium (DMEM) containing with 10% FBS at 37 ℃ in a CO_2 incubator (Thermo Fisher Scientific, Waltham, MA, USA) under 5% CO_2.

2.3. Extraction and gelation of bamboo fungus protein

Extraction and gelation of bamboo fungus proteins according to a previous report (Zhang et al., 2021). Briefly, defatted bamboo fungus powders were extracted at 50 °C using deionized water (1:20 g/mL, pH 9) for 2.5 h. The upper phase was obtained by centrifugation, adjusted to pH 4.5 and then at 4 °C overnight. Protein precipitate was collected, washed and dispersed with deionized water, transferred to a dialysis bag and processed for 24 h. Finally, the proteins were lyophilized and stored at 4 °C. Enzyme-induced gelation operations were as follows: Bamboo fungus protein solution (15%, *w/v*) was prepared with deionized water, preheated at 85 °C for 20 min, and cooled down to room temperature, then mixed with transglutaminase (20 U/g). Subsequently, the mixture was undergone enzymatic reaction at 50 °C for 4 h to form protein gels. Finally, the protein gels were refined with high-speed shearing. Gel dispersions (5%, *w/v*) were further prepared with deionized water and homogenized (HR-6, Rotor diameter: 5 mm, Shanghai, China) for 5 min at 10,000 rpm to obtain BGPs for the following steps.

2.4. KO-HIPPE preparation

KO and soybean oil were mixed (0:10 to 3:7, *v/v*) at 100 rpm for 10 min as the oil phase. Different pH (3 or 11) and concentration (0.5, 1 and 2%, *w/v*) of BGPs dispersions was blended with oil phase, the volume ratio of 1:4 ($\varphi = 80\%$). Samples were emulsified at 10,000 rpm for 1.5 min, then the KO-HIPPE was manufactured and stored at 4 °C for further study.

2.5. Structures and properties of KO-HIPPE

2.5.1. Structural characterization of KO-HIPPE

Samples with the corresponding pH aqueous solutions were diluted. Droplet size and ζ-potential of the KO-HIPPE at different pH values were determined by a Zetasizer Nano ZS90 (Malvern, U.K.). Measurement temperature: 25 °C, Dispersant RI: 1.330, Material RI:1.480, Material Absorbtion: 0.001. Measurement angle: 90°. The confocal laser scanning microscopy (CLSM) images were taken at 488 nm (C2 + confocal microscope Nikon, Japan) after staining of KO-HIPPE (1.0 wt% Nile Red dissolved in isopropyl alcohol).

2.5.2. Storage stability of KO-HIPPE

KO-HIPPE sample was placed in a corked sample bottle and stored at 4 °C. Storage stability was assessed based on the changes in droplet size distribution using visual and microstructural observations (Hao, Peng, & Tang, 2020). The appearance of KO-HIPPE was recorded weekly. Meanwhile, the droplet size of the emulsion was determined by Zetasizer Nano ZS90, all test samples were picked from the upper layer of KO-HIPPE.

2.6. Digestive features of KO-HIPPE

The *in vitro* digestion method was according to a previous study (Liu et al., 2019), with some modifications. In brief, 7.5 mL sample solutions were prepared by blending 3.75 mL KO-HIPPE (C = 1.0%, pH = 11) or 3 mL oil phase with ionized water, respectively. 0.5 M HCl or 0.5 M NaOH solution were used to adjust the pH of digestion fluid. Prior to the experiment, all sample and simulated digestion solutions were pre-heated to 37 °C. *Mouth stage*: 7.5 mL of sample solution was mixed with 7.5 mL of simulated saliva fluid (SSF) containing 30 mg/mL mucin, then the mixture was adjusted to pH 6.8 and simulated digestion at 37 °C for 10 min at 100 rpm (water bath thermostatic shaker SHA-C, Changzhou, China). *Gastric stage*: 15 mL of oral digesta was mixed with 15 mL of simulated gastric fluid (SGF) containing pepsin (3.2 mg/mL), HCl (7 mL/L) and NaCl (2 mg/mL). Subsequently, digestion pH was adjusted to 2.5 and digested at 37 °C, 100 rpm for 2 h. *Small intestine stage*: Simulated intestinal fluid (SIF) contained 3.5 mL bile salt solution (54 mg/mL), salt solution (218.7 mg/mL NaCl, 36.7 mg/mL $CaCl_2$), 2.5 mL lipase (24 mg/mL) and trypsin (24 mg/mL). The enzyme and bile salts were dissolved in PBS solution (5 mM, pH 7). After SIF added to 30 mL of stomach digesta, the system was adjusted to pH 7 and maintained at 37 °C and 100 rpm for 2 h. During digestion, the pH of the system was maintained at 7 with 0.2 M NaOH solution for 10 min intervals, and FFA release was calculated based on the consumed volume of NaOH.

2.7. Anti-inflammatory activity of KO-HIPPE in vitro

2.7.1. Cell viability assay

Cell viability assay based on previous methods with modifications (Zhou et al., 2021a). RAW 264.7 cells were seeded in 96-well plates at a density of 5×10^4 cells/well and incubated for 24 h. Work solutions included KO-HIPPE or mixed oils (KO and soybean oil, 2:8 *v/v*) at concentrations of 0, 0.0625, 0.125, 0.25, 0.5, and 1 mg/mL diluted by serum-free medium, while LPS (0, 1 μg/mL) was added. Cells were treated with work solution for 24 h, then, the wells were washed with PBS, incubated with MTT reagent (0.5 mg/mL) for 4 h. Supernatants were removed, 150 μL DMSO was added to dissolve the formazan crystals in each well, and the absorbance at 570 nm was measured using microplate reader (Tecan Spark 10 M, Männedorf, Switzerland). Cell viability was calculated using the following formula: %Cell viability = (A1/A0) × 100%, where A1 and A0 were the absorbances of the test samples and control, respectively.

2.7.2. Determination of NO production

Cells were seeded and incubated as described above. Then, RAW 264.7 cells were grouped, normal group: administered with serum-free medium; LPS group: administered with 1 μg/mL LPS solution, KO-HIPPE group: administered with both 1 μg/mL LPS and KO-HIPPE (0, 0.0625, 0.125, 0.25, 0.5, and 1 mg/mL) work solutions. After 18 h of treatment, Griess method was used to determine NO production. No inhibition rate = ($OD_{\text{LPS group}}$ - $OD_{\text{KO-HIPPE group}}$) / ($OD_{\text{LPS group}}$ - $OD_{\text{normal group}}$) × 100%.

2.8. Anti-inflammatory activity of KO-HIPPE on DSS-induced colitis mice

2.8.1. Animal experimental design

C57BL/6 mice were randomly divided into five groups (n = 10): normal group, DSS group and KO-HIPPE group (L-KO-HIPPE: 200 mg/kg, M−KO−HIPPE: 400 mg/kg and H-KO-HIPPE: 800 mg/kg). Physiological saline was given to the normal group, DSS (3.0%, dissolved in physiological saline) was given to the other groups and free drinking to induce ulcerative colitis (UC). Meanwhile, KO-HIPPE group was treated with different doses of KO-HIPPE daily for 9 days by intragastric administration, normal and DSS groups were treated with saline.

2.8.2. Calculation of disease activity index (DAI)

Mice weight changes, stool characteristics and fecal occult blood were recorded daily. Based on the above recording and scoring system (Table S1), DAI was finally calculated.

2.8.3. Sample collection

After 9 days of administration, all mice were sacrificed with anesthesia. Serum, colon, spleen, and liver were collected immediately. Colons were photographed and colon length, spleen weights were recorded. Tissue and organ samples were rapidly frozen in liquid nitrogen and then transferred to −80 °C storage for subsequent experiments. After cleaning colonic contents using saline, same colonic sections were fixed using 4% paraformaldehyde, embedded in paraffin and stained with hematoxylin and eosin (H&E). Histopathology scores were assessed according to Table S2. Splenic index was obtained by dividing the weight of the spleen with the corresponding body weight.

2.8.4. Determination of TNF-α and IL-6 levels

Fresh blood was placed at room temperature for 2 h and then centrifuged at 4 °C to obtain serum. The content of TNF-α and IL-6 in mice serum was determined according to the ELISA kit instructions.

2.8.5. Measurement of oxidative stress

The colon tissue was cleaned and ground to produce homogenate, followed by the centrifugation (3500 rpm, 10 min) at 4 °C to obtain supernatant. The malondialdehyde (MDA) content was determined from the homogenate, while the glutathione (GSH), superoxide dismutase (SOD) and protein content was determined from the supernatant. All operations were performed in accordance with the kit instructions.

2.8.6. Western blot analysis

Colon tissue was washed and made into homogenate, 1 mL of RIPA lysis solution (containing protease 1:100 and 0.1 M EDTA) was added and lysed on ice for 1 h. Supernatant was obtained by centrifugation and subsequent processes were carried out according to previous study (Zhou et al., 2021a).

2.9. Statistical analyses

All measurements were performed in triplicate, and data were expressed as mean ± standard deviation. Multiple comparisons were analyzed using one-way analysis of variance (ANOVA) and then Tukey's post hoc test. Statistical analysis and plotting were done by GraphPad Prism 8 and SPSS 16.0, statistical significance was set at $P < 0.05$.

3. Results and discussion

3.1. KO-HIPPE preparation and composition optimization

The appearance of KO-HIPPE prepared with different compositions at pH 3 and 11 were shown in Fig. 1a and Fig. 1b. The droplets size and ζ-potential of KO-HIPPE were given in Table S3. Obviously, KO-HIPPE cannot be established in the absence (0:10) or a small amount of KO (1:9). But with the increasing proportion of KO (2:8) in oil phase, the system stability was clearly improved, which may attribute to the high level PLs in KO. Natural surfactants interact with protein particles at phase interface, at low concentrations, amphiphilic molecules enter the spaces between protein particles, reducing interfacial tension and

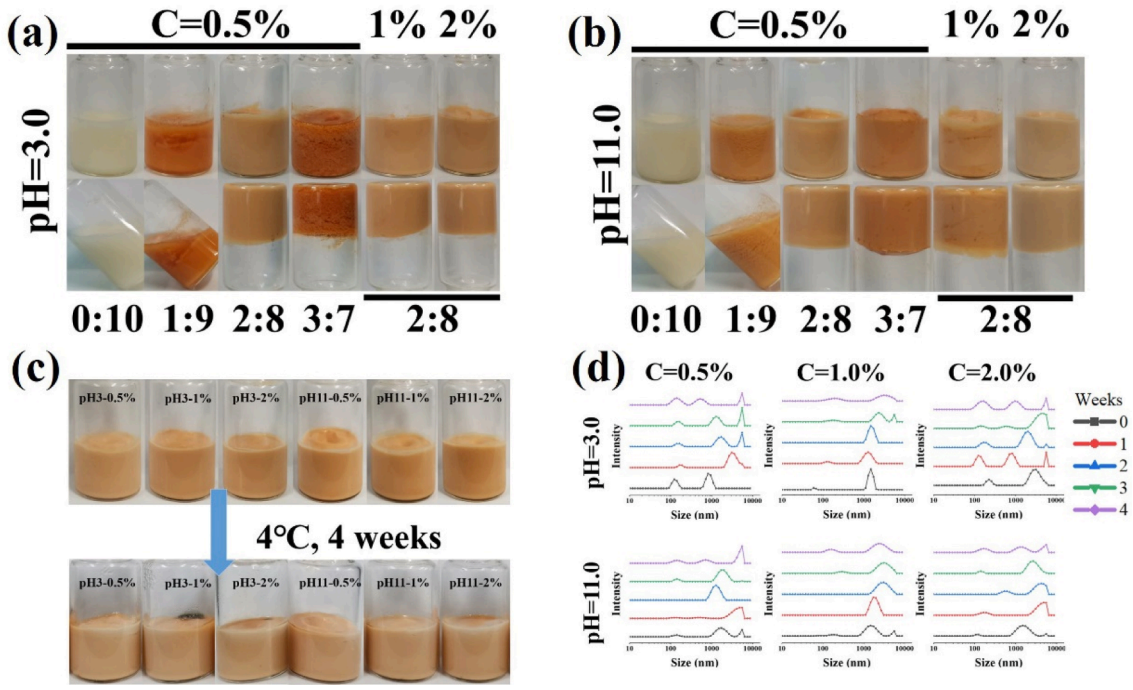

Fig. 1. The appearance of the KO-HIPPE with different compositions. (a) pH = 3, (b) pH = 11; The appearance and particle size development of KO-HIPPE during storage at 4 °C. (c) Appearance photos, (d) Droplet size distribution curve.

promoting emulsion stability. In contrast, at high concentrations, competitive adsorption between surfactants and particles occurs on the droplet surface, destroying the original physical barrier and leading to destabilization (Wei et al., 2020). This explained the phenomenon that KO-HIPPE were stabilized in 2:8 oil phase composition while unstable in 3:7 at pH 3.0 under the same conditions. As for an oil phase composition of 3:7, compared to pH 3.0, KO-HIPPE at pH 11.0 under the same conditions can be stabilized due to the higher electrostatic interactions that maintain system stability (Table S3). Lower absolute potential means weaker electrostatic repulsion and the emulsion tends to become unstable (Zhang et al., 2021). At oil phase composition of 2:8, KO-HIPPE could be stabilized regardless of the stabilizer concentration. However, 2.0% BGPs resulted in certain increased size of the KO-HIPPE (Table S3) due to the excessive, unabsorbed stabilizer may have a depletion effect, resulting in flocculation and aggregation of emulsion droplets (Gao et al., 2017).

3.2. Microstructures and properties of KO-HIPPE

3.2.1. Microstructure of KO-HIPPE

The KO-HIPPE (pH 11, 1.0%, 2:8) microstructure was shown in Fig. S1a, the droplets were intact spheres with uniform particle size about 1.5 μm, the result was in accordance with Table 1. CLSM image revealed that the oil phase was encapsulated in the droplet and no leakage occurred (Fig. S1b). Previous studies demonstrated that the BGPs formed an interfacial film which were tightly wrapped around the oil droplets, and the physical barrier and electrostatic repulsion were the main drivers for HIPPE stabilization (Zhang et al., 2021). Pickering emulsions stabilized by several types of stabilizers exhibited the same structural characteristics in recent reports (Sharkawy, Barreiro, & Rodrigues, 2022; Sharkawy, Barreiro, & Rodrigues, 2019). Interestingly, just altering the oil phase type resulted in a large difference in particle size (15.85 μm to 1.5 μm). Oil phase properties, such as polarity, molecular weight, surface tension, viscosity, etc. had impacts on the physicochemical characteristics of the emulsion (Taha et al., 2018). HIPPE composed of isooctane or mixed oils could be stabilized by BGPs, despite the color and size differences. Herein, BGPs exhibited potential application capabilities.

3.2.2. Stability of KO-HIPPE

Fixed oil phase composition ratio of 2:8, different concentrations and pH of KO-HIPPE participated in stability assessment. The appearance and particle size development during storage at 4 °C were shown in Fig. 1c. After 4 weeks, the appearance of KO-HIPPE remained stable without significant changes, indicating a high coalescence stability against a long-term storage (Hao et al., 2020). According to the droplet size distribution curve (Fig. 1d), the KO-HIPPE before storage showed a double peak distribution for all preparation conditions. The first peak was located in the range of 100–200 nm which resulted from the unabsorbed BGPs. The particle size of dispersed BPGs in previous study was 227 nm (Zhang et al., 2021). The second peak was the dominant one, located in the range of 1–3 μm, reflecting the main droplet size of the KO-HIPPE. With prolonged storage time, the size of all KO-HIPPE was changed during storage due to Ostwald ripening and aggregation, leading to the appearance of a third peak, located at 5 μm, and a rightward shift of the main peak. The above phenomenon indicated that a part of the droplets merged and the particle size increased until large droplets formed. Comparing the changes of each KO-HIPPE size distribution curve during storage, the pH = 11, C = 1.0% KO-HIPPE showed better storage stability as third peak didn't appeared after 4 weeks storage. In general, excellent storage stability derived from their structure was a characteristic present in most HIPPE (Li et al., 2020a).

3.2.3. In vitro digestion

As shown in Fig. 2a, microstructure of KO-HIPPE were significantly changed with different digestion sites. After oral digestion, KO-HIPPE had a uniform size distribution and droplets approach each other. There was no significant change in the ζ-potential at this site, but a slight increase in size (Fig. 2b and Fig. 2c), which was due to droplets flocculation and coalescence of mucin induced during mouth stage owing to depletion and bridging mechanisms (Li et al., 2020b). Obviously, at the end of gastric stage, KO-HIPPE size became inhomogeneous and some large droplets appeared. Low pH value of the digest and salt ions caused an increase of ζ-potential from −62 mV to −30 mV, which indicated that

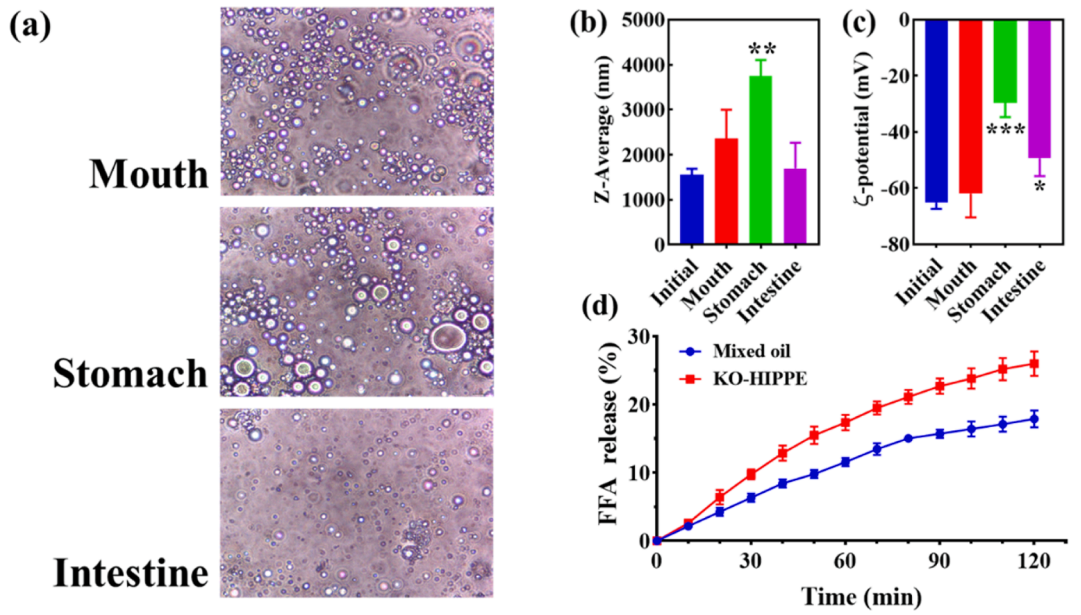

Fig. 2. Microstructure and property of the KO-HIPPE in different digestion sites. (a) Microscopic images, (b) Droplet size, (c) zeta potential, (d) FFA release profiles. *$P < 0.05$ vs Initial.

the electrostatic interaction forces were weakened, leading to flocculation and coalescence (Zhang et al., 2021). On the other hand, physical barrier constituted by BGPs was destroyed by pepsin, which also caused an increase in size (Araiza-Calahorra, Glover, Akhtar, & Sarkar, 2020). During small intestine stage, a decrease of droplet number and size was observed. This indicated that KO-HIPPE were digested by the combined action of pepsin, pancreatin and lipase, and large droplets in the previous digestion phase thus disappeared. Meanwhile, the products of oil digestion combined with substances in the digestive solution such as bile salts produced calcium soaps, micelles and vesicles, which caused the decrease of the size of the emulsion (Li et al., 2020b).

3.2.4. FFA release

FFA release profiles of KO-HIPPE and mixed oil during simulated intestinal digestion were shown in Fig. 2d. Obviously, KO-HIPPE showed a faster and more complete release of FFA (25.98% > 17.89%). Lipid digestion was a bio-interfacial process which was dependent on the attachment of the lipase enzyme-colipase-biosurfactant (bile salts) complex at the o/w interface (Nikbakht Nasrabadi, Sedaghat Doost, Goli, & Van der Meeren, 2020). Compared to mixed oil, KO-HIPPE droplets had a larger surface area in containing the same amount of oil, which provided more lipase binding sites and improved the reaction efficiency (Huang et al., 2021; Wei, Cheng, Zhu, & Huang, 2019). Similar reports confirmed that as the droplet diameter decreased, the surface area of the lipid phase exposed to pancreatic, lipase and bile salts increased, and ultimately the rate of lipolysis and the degree of lipolysis tended to increase (Wei, Cheng, & Huang, 2019; Yi et al., 2020). In addition, certain types of Pickering nanoparticle stabilizers located at the oil–water interface resisted the competitive replacement of bile salts and delayed the translocation of lipase (Santos et al., 2021). However, for BGPs, which were suffered from the proteases during the digestion, the interface membrane formed by BGPs became weak, resulting in its inability to prevent lipase transfer and binding.

3.3. Anti-inflammatory activity in vitro

3.3.1. Effect of KO-HIPPE on the macrophage viability

RAW 264.7 are mice macrophages that play a critical role in the inflammatory response as primary immune cells. Upon stimulation by specific substances such as LPS, various inflammatory mediators including cyclooxygenase 2 (COX-2), nitric oxide (NO), prostaglandin E_2, various cytokines and chemokines were produced to induce inflammatory responses (Qian et al., 2021). This cellular model of inflammatory response was widely used to evaluate the anti-inflammatory immune activity of drugs (Liu, Li, Guo, & Zhang, 2020b). For unstimulated cells (0.25 mg/mL), the cell viability was 58.25% in the mixed oil sample and 90.69% in the KO-HIPPE sample (Fig. 3a). At higher concentrations (0.5 and 1 mg/mL), cell viability was only 9.70% in the mixed oil sample but remained above 70% in the KO-HIPPE sample. As for LPS-stimulated cells, mixed oil at high concentrations (0.5 and 1 mg/mL) also caused a low cell viability of 6.22%, while KO-HIPPE remained above 70% (Fig. 3b). The excessive accumulation of lipids in cells after intake of high concentrations of fatty acids can lead to impaired cell function and even apoptosis, a phenomenon known as lipid toxicity. It can explain the phenomenon that high concentration of mixed oils led to the decrease of cell viability (Piccolis et al., 2019). Furthermore, Pickering emulsions with complex interfacial structures have been shown to reduce the effects of excess encapsulated substances on cell viability (Araiza-Calahorra, Wang, Boesch, Zhao, & Sarkar, 2020). All in all, the results demonstrated that KO-HIPPE had no cytotoxicity effect on RAW 264.7 cells which can be used in cellular testing with no>0.25 mg/mL.

3.3.2. Effect of KO-HIPPE on productions of NO

NO is a biologically functional free radical and excessive production can lead to inflammation. As shown in Fig. 3c, NO production was inhibited after treatment KO-HIPPE for 18 h. The NO inhibition rate was dose-dependent, with the highest inhibition rate of 32.84% at 0.25 mg/mL. Higher doses of KO-HIPPE (0.5 and 1 mg/mL) led to a decrease in cell viability and thus NO production and were not discussed. The result was in agreement with previous study (Zhou et al., 2021a). The anti-inflammatory activities of KO-HIPPE might be attributed to PLs and omega-3 fatty acids. PLs in KO bound to and neutralized endotoxin LPS, thus preventing macrophage activation and inflammatory mediator release. And omega-3 fatty acids regulated eicosanoid metabolism, exhibiting a positive synergistic effect with PLs (Bonaterra, Driscoll, Schwarzbach, & Kinscherf, 2017).

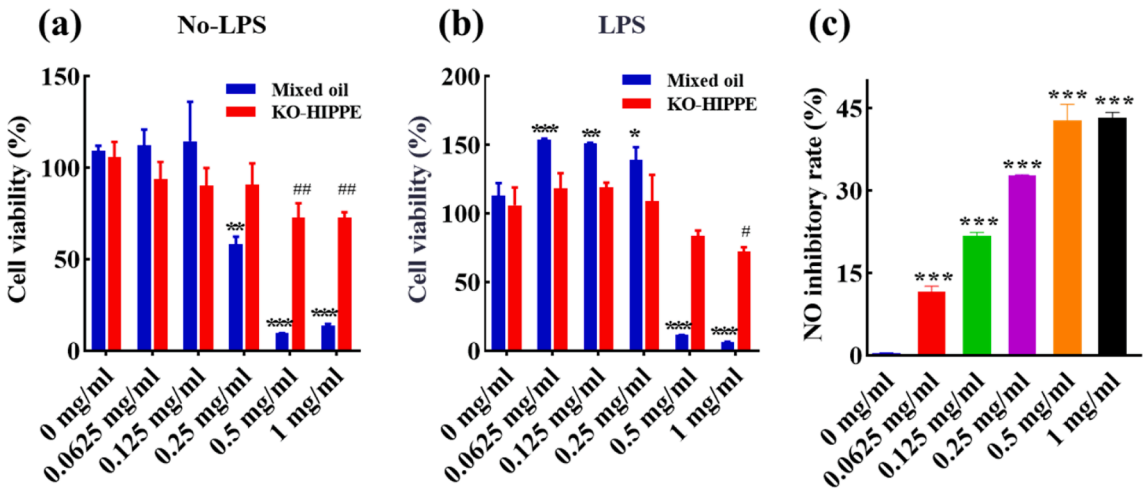

Fig. 3. Effect of KO-HIPPE on cell viability and NO production in RAW.264.7 cells. (a) Cell viability in treated with LPS group, (b) Cell viability in no treated with LPS group, (c) NO production. *$P < 0.05$ vs 0 mg/mL group, #$P < 0.05$ vs 0 mg/mL group.

3.4. Anti-inflammatory activity of KO-HIPPE on DSS-induced colitis mice

3.4.1. KO-HIPPE alleviated the UC symptoms

DSS-induced colitis mice were widely used because of its simplicity and many similarities to human colitis, including weight loss, fecal bleeding and loose stools, severity of which can be expressed by DAI (Chassaing, Aitken, Malleshappa, & Vijay-Kumar, 2014). As shown in Fig. 4a and Fig. 4b, all mice treated with DSS showed a significant increase of DAI and decrease of body weight. The generation and development of these symptoms indicated the successful establishment of UC model. After 9 days of administration KO-HIPPE, weight loss was reduced (L-KO-HIPPE: 17.6%, M−KO−HIPPE: 17.9% and H-KO-HIPPE: 15.9%) compared to the DSS group (23.5%). Meanwhile, DAI slightly decreased in KO-HIPPE group compared with the DSS group. Same trends were observed in KO liposome treatment of colitis (Kim et al., 2019).

The colon length of the DSS group was significantly shortened (Fig. 4c and d). The colonic length of the KO-HIPPE group was restored after the administration of KO-HIPPE. As an important immune organ, spleen was enlarged and darkened when the inflammatory response occurred in the body (Chassaing et al., 2014). Spleen index of mice was shown in Fig. 4e, DSS group showed a significant increase compared with normal group (0.7472 vs 0.3049). After KO-HIPPE administration, the spleen index was reduced (L-KO-HIPPE: 0.6447, M−KO−HIPPE: 0.6049 and H-KO-HIPPE: 0.6176), indicating KO-HIPPE can reduce DSS-induced splenic damage. It indicated that KO-HIPPE can alleviate the symptoms of DSS-induced UC in mice. These results were consistent with a previous literature (Zhou et al., 2021b), which revealed the positive effect of KO interventions for DSS-induced colitis mice.

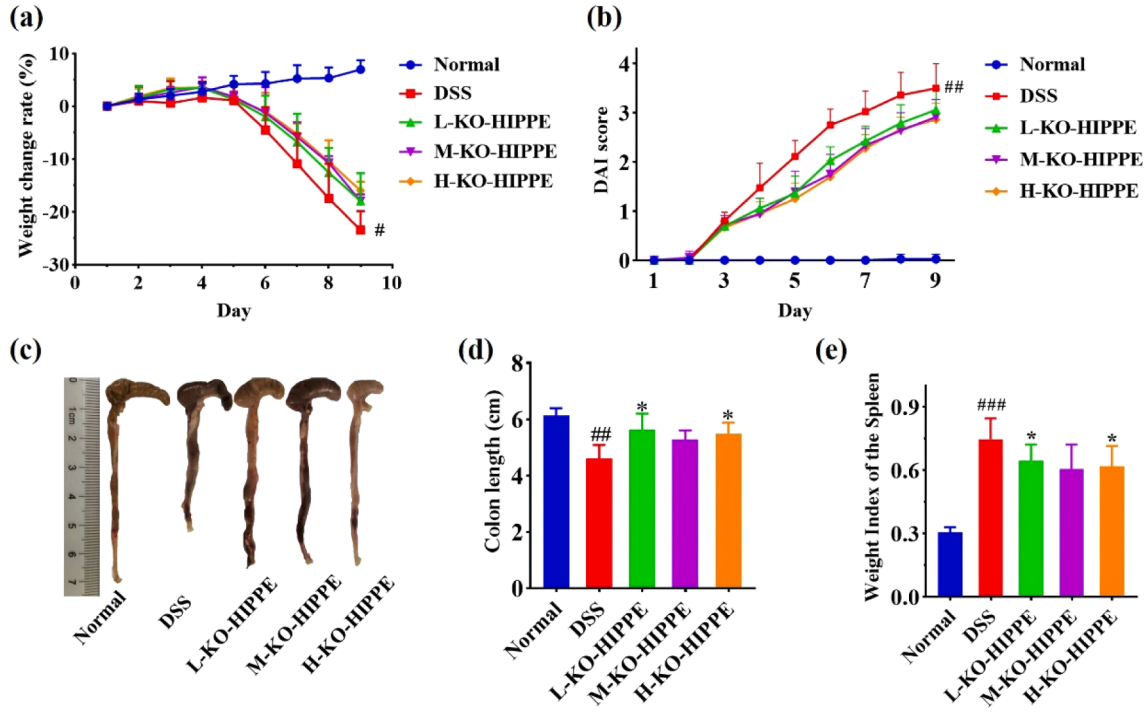

Fig. 4. Effect of KO-HIPPE on DAI and body weight change in DSS-induced UC mice. (a) Body weight change, (b) DAI development; Effect of KO-HIPPE on organs and tissues in DSS-induced UC mice. (c) Colon appearance photos, (d) colon length, (e) Spleen weight index. #$P < 0.05$ vs normal group, *$P < 0.05$ vs DSS group.

3.4.2. Effects of KO-HIPPE on histological changes of intestinal tissue

Intestinal mucosal barrier mainly consists of the mucus layer, epithelial layer, lamina propria and components such as intestinal microbiota, anti-microbial peptides and immune cells (Wu, Wei, Wang, Qi, & Wang, 2018). H&E staining was used to evaluate the histological characteristics of the mice colon. In the normal group, the colonic epithelium was intact with normal morphology, the intestinal glands were tightly arranged without inflammatory edema (Fig. 5a). In contrast, the structure of colon tissues was clearly altered in DSS group, which exhibited widespread inflammatory infiltration and glandular loss, disappearance of most crypt and goblet cells, destruction of epithelial layer, and significant increase of histological scores (Fig. 5b). It indicated successful establishment of the UC model (Chassaing et al., 2014). After the treatment with different doses of KO-HIPPE, colonic inflammation was relieved, epithelial cells were more intact relative to the model group, glands and crypt were protected, and histological scores were significantly decreased. Similarly, KO significantly increased the number of goblet cells, and colonic smooth muscle thickness and overall histopathological scores were improved in Th2-driven porcine colitis model (Liu et al., 2020a). Phosphatidylcholine rich in KO bound to the mucin of the colonic mucus, creating a protective surface that prevented adhesion and penetration of potentially toxic antigens. Furthermore, omega-3 fatty acids could reduce colonic damage and inflammation through fatty acid entry into cell membranes and reduce the activation of pro-inflammatory transcription factors (Kim et al., 2019).

Intestinal epithelial cells connected with each other by tight junction proteins including occludin, ZO-1 and claudin which regulated the paracellular permeability (Wu et al., 2018). As shown in Fig. 5c and 5d, KO-HIPPE treatment significantly inhibited the decrease of occludin induced by DSS, the result was consistent with histopathological observations (Fig. 5a). Similarity, the exposure of HT29 and CACO2 to pro-inflammatory cytokines resulted in a strong reduction in tight junction proteins expression, which was significantly restored after KO treatment (Costanzo et al., 2016). All in all, the results demonstrated that KO-HIPPE could improve DSS-induced colon injury.

3.4.3. Effect of KO-HIPPE on the production of cytokines

Intestinal epithelial cells were disrupted owing to apoptotic foci and altered expression of tight junction proteins, thus permitted more microbiota to cross the barrier, activate macrophages and antigen presenting cells, ultimately led to the production of tumor necrosis factor (TNF), IL-12, IL-23 and IL-6 (Kobayashi et al., 2020). TNF-α and IL-6 levels in serum were measured by ELISA and the results were shown in Fig. 6a and b. TNF-α and IL-6 levels were significantly higher in the DSS group compared with the normal group (TNF-α: 1053 pg/mL vs 184.0 pg/mL, IL-6: 689.4 pg/mL vs 107.2 pg/mL), indicating DSS induction caused colonic inflammation. These pro-inflammatory factors levels were significantly decreased after KO-HIPPE treatment (TNF-α: 261.9, 191.6 and 260.2 pg/mL; IL-6: 252.9, 244.5, 234.9 pg/mL). Similarly, KO liposomes significantly reduced serum TNF-α and IL-6 levels in UC mice (Kim et al., 2019).

3.4.4. Effect of KO-HIPPE on antioxidant enzyme activities and malondialdehyde levels

MDA is a result of lipid peroxidation and has been used as a marker of oxidative stress during UC, because the inflammation leads to the increase of MDA in colonic tissue (Pavan et al., 2021). As shown in Fig. 6c, compared with model group, KO-HIPPE could reduce the MDA content in the colon significantly ($P < 0.05$). In particular, administration of 400 mg/kg KO-HIPPE could decrease MDA content more effectively, from 93.53 to 47.54 nmol/mg protein. GSH, as a scavenger of ROS, played an important role in control cellular redox conditions, and its depletion was a feature of colitis (Pavan et al., 2021). When the inflammation occurred, the GSH content of the model group decreased significantly to 10.92 μmol/g protein, after 400 mg/kg KO-HIPPE treatment, it returned to 16.09 μmol/g protein, was close to the level of the normal group (Fig. 6d). The change trend of SOD scavenging oxygen radical activity was similar with GSH. Inflammation led to a decrease in SOD activity (55.98 U/mg protein), and 200 or 400 mg/kg KO-HIPPE treatment was able to maintain SOD activity (71.39 and 82.81 U/mg protein) (Fig. 6e). KO exhibited the same trend in PC 12 cells when oxidative damage occurred, it was probably attributed to the presence of abundant astaxanthin in KO (Xiong et al., 2018).

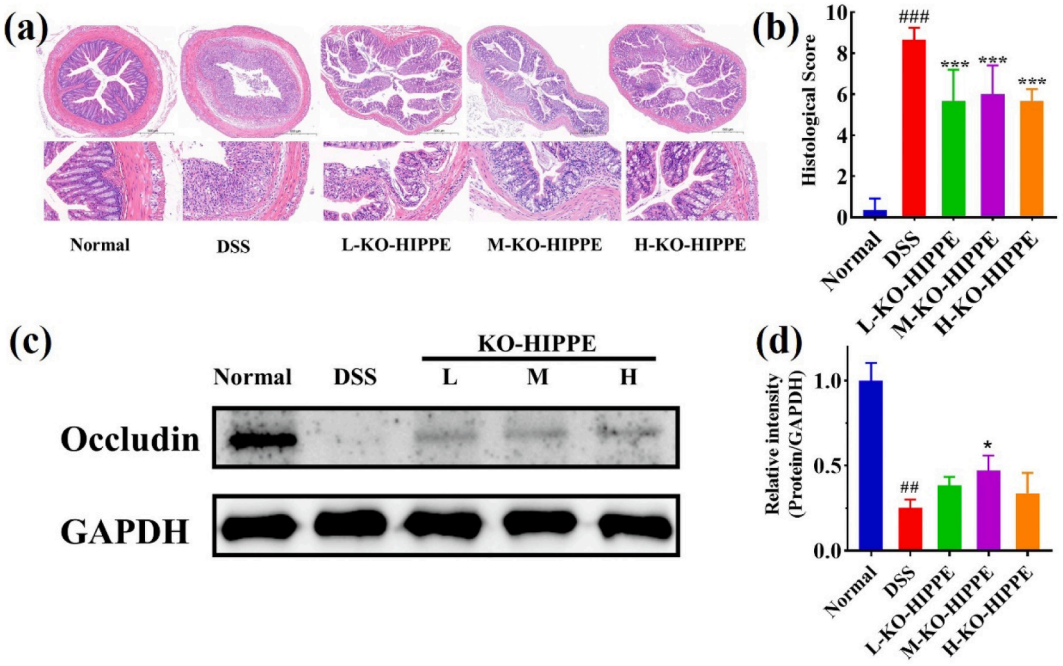

Fig. 5. Effect of KO-HIPPE on colon injury in DSS-induced UC mice. (a) HE stained images of colon tissue, (b) Colon histopathology score, (c) Protein bands analysis, (d) Relative content of occludin. #$P < 0.05$ vs normal group, *$P < 0.05$ vs DSS group.

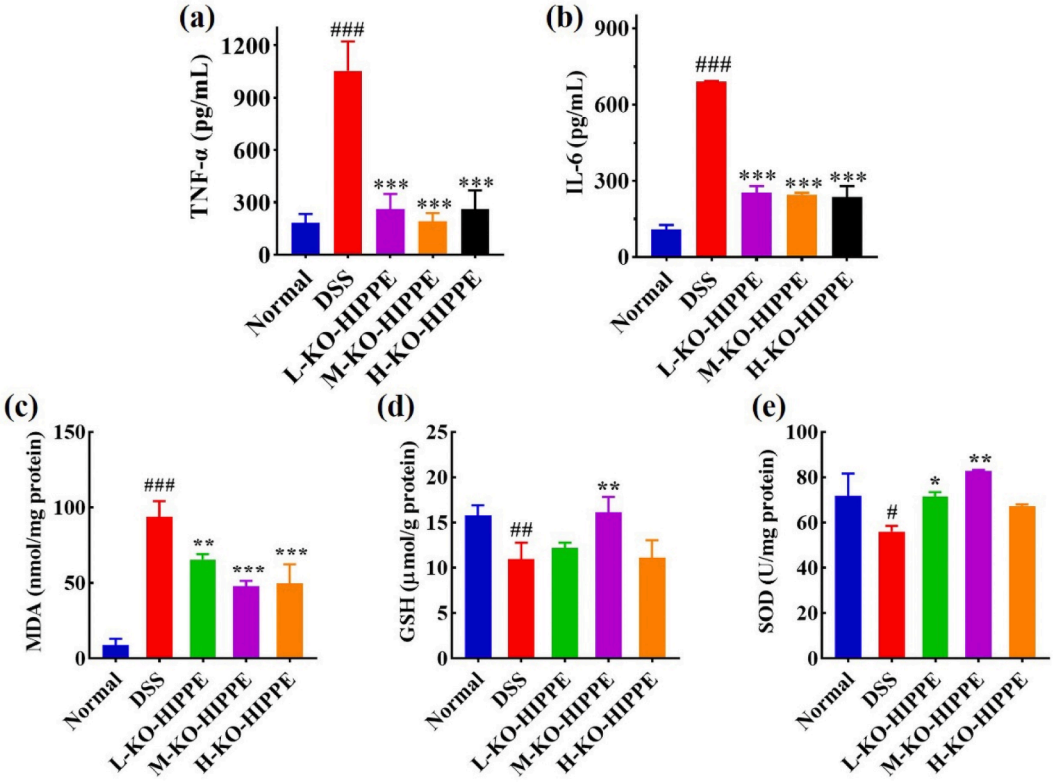

Fig. 6. Effect of KO-HIPPE on serum proinflammatory cytokines in DSS-induced UC mice. (a) TNF- α, (b) IL-6; Effect of KO-HIPPE on colonic tissue oxidative stress in DSS-induced UC mice. (c) MDA content, (d) GSH content, (e) SOD activity $\#P < 0.05$ vs normal group, $*P < 0.05$ vs DSS group.

4. Conclusion

In the present study, KO-HIPPE stabilized by BGPs were successfully prepared. KO-HIPPE showed excellent storage stability, remaining stable at 4℃ for at least 4 weeks. When KO encapsulated, it exhibited faster and more complete digestion characteristics *in vitro* compared to mixed oil. Moreover, *in vitro* and *in vivo* anti-inflammatory activity of KO-HIPPE were investigated. For RAW 264.7 cell, 0.25 mg/mL KO-HIPPE had no effect on cell viability and the NO inhibition (32.84%), suggested its safety and anti-inflammatory effect. For UC mice, KO-HIPPE treatment reduced the DAI and attenuated clinical symptoms, prevented the reduction of occludin in colonic tissue and protected the intestinal barrier with function. Meanwhile, KO-HIPPE showed a modulating effect on the inflammatory response and modulated oxidative stress and suppressed the overexpression of the pro-inflammatory cytokines (TNF-α and IL-6). The study suggested that BGPs stabilized HIPPE can effectively encapsulate and deliver of KO to improve human health by modulating the host immunoreaction.

CRediT authorship contribution statement

Minghao Zhang: Writing – review & editing. **Jinrui Zhu:** Investigation. **Li Zhou:** Supervision, Writing – review & editing. **Jianquan Kan:** Visualization, Investigation. **Minjie Zhao:** . **Rong Huang:** Investigation. **Jikai Liu:** . **Eric Marchioni:** Investigation.

Declaration of Competing Interest

The authors declare that they have no known competing financial interests or personal relationships that could have appeared to influence the work reported in this paper.

Acknowledgements

This work received supports from the National Natural Science Foundation of China (31501521) and the Fundamental Research Funds for the Central Universities, the South-Central University for Nationalities (CZY19032).

Appendix A. Supplementary material

Supplementary data to this article can be found online at https://doi.org/10.1016/j.jff.2022.105134.

References

Zhou, L., Wu, X., Yang, F., Zhang, M., Huang, R., & Liu, J. (2021a). Characterization of molecular species and anti-inflammatory activity of purified phospholipids from Antarctic krill oil. *Marine Drugs, 19*(3), 1–15. https://doi.org/10.3390/md19030124

Zhou, X., Xiang, X., Zhou, Y., Zhou, T., Deng, S., Zheng, B., & Zheng, P. (2021b). Protective effects of Antarctic krill oil in dextran sulfate sodium-induced ulcerative colitis mice. *Journal of Functional Foods, 79*, 1–13. https://doi.org/10.1016/j.jff.2021.104394

Araiza-Calahorra, A., Glover, Z. J., Akhtar, M., & Sarkar, A. (2020). Conjugate microgel-stabilized Pickering emulsions: Role in delaying gastric digestion. *Food Hydrocolloids, 105*, 1–13. https://doi.org/10.1016/j.foodhyd.2020.105794

Araiza-Calahorra, A., Wang, Y., Boesch, C., Zhao, Y., & Sarkar, A. (2020). Pickering emulsions stabilized by colloidal gel particles complexed or conjugated with biopolymers to enhance bioaccessibility and cellular uptake of curcumin. *Curr Res Food Sci, 3*, 178–188. https://doi.org/10.1016/j.crfs.2020.05.001

Bonaterra, G. A., Driscoll, D., Schwarzbach, H., & Kinscherf, R. (2017). Krill Oil-In-Water Emulsion Protects against Lipopolysaccharide-induced proinflammatory activation of macrophages *in vitro*. *Marine Drugs, 15*(3), 1–12. https://doi.org/10.3390/md15030074

Chassaing, B., Aitken, J. D., Malleshappa, M., & Vijay-Kumar, M. (2014). Dextran sulfate sodium (DSS)-induced colitis in mice. *Current Protocol Immunology, 104*, 1–15. https://doi.org/10.1002/0471142735.im1525s104

Choi, J. Y., Jang, J. S., Son, D. J., Im, H. S., Kim, J. Y., Park, J. E., … Hong, J. T. (2017). Antarctic krill oil diet protects against lipopolysaccharide-induced oxidative stress, neuroinflammation and cognitive impairment. *International Journal of Molecular Sciences, 18*(12), 1–15. https://doi.org/10.3390/ijms18122554

Costanzo, M., Cesi, V., Prete, E., Negroni, A., Palone, F., Cucchiara, S., … Stronati, L. (2016). Krill oil reduces intestinal inflammation by improving epithelial integrity and impairing adherent-invasive Escherichia coli pathogenicity. *Dig Liver Dis, 48*(1), 34–42. https://doi.org/10.1016/j.dld.2015.09.012

Feng, X., Sun, Y., Yang, Y., Zhou, X., Cen, K., Yu, C., … Tang, X. (2020). Zein nanoparticle stabilized Pickering emulsion enriched with cinnamon oil and its effects on pound cakes. *LWT-Food Science Technology, 122*, 1–9. https://doi.org/10.1016/j.lwt.2020.109025

Gao, Z. M., Zhao, J. J., Huang, Y., Yao, X. L., Zhang, K., Fang, Y. P., … Yang, H. (2017). Edible Pickering emulsion stabilized by protein fibrils. Part 1: Effects of pH and fibrils concentration. *LWT-Food Science Technology, 76*, 1–8. https://doi.org/10.1016/j.lwt.2016.10.038

Hao, Z. Z., Peng, X. Q., & Tang, C. H. (2020). Edible pickering high internal phase emulsions stabilized by soy glycinin: Improvement of emulsification performance and pickering stabilization by glycation with soy polysaccharide. *Food Hydrocolloids, 103*, 1–9. https://doi.org/10.1016/j.foodhyd.2020.105672

Huang, M., Wang, Y., Ahmad, M., Ying, R., Wang, Y., & Tan, C. (2021). Fabrication of pickering high internal phase emulsions stabilized by pecan protein/xanthan gum for enhanced stability and bioaccessibility of quercetin. *Food Chemistry, 357*, 1–9. https://doi.org/10.1016/j.foodchem.2021.129732

Huang, X. N., Zhu, J. J., Xi, Y. K., Yin, S. W., Ngai, T., & Yang, X. Q. (2019). Protein-based pickering high internal phase emulsions as nutraceutical vehicles of and the template for advanced materials: A perspective paper. *Journal of Agriculture and Food Chemistry, 67*(35), 9719–9726. https://doi.org/10.1021/acs.jafc.9b03356

Jafari, S. M., Doost, A. S., Nasrabadi, M. N., Boostani, S., & Van der Meeren, P. (2020). Phytoparticles for the stabilization of Pickering emulsions in the formulation of novel food colloidal dispersions. *Trends in Food Science & Technology, 98*, 117–128. https://doi.org/10.1016/j.tifs.2020.02.008

Jiao, B., Shi, A., Wang, Q., & Binks, B. P. (2018). High-internal-phase Pickering emulsions stabilized solely by peanut-protein-isolate microgel particles with multiple potential applications. *Angewandte Chemie (International ed. in English), 57*(30), 9274–9278. https://doi.org/10.1002/anie.201801350

Kim, J. H., Hong, S. S., Lee, M., Lee, E. H., Rhee, I., Chang, S. Y., & Lim, S. J. (2019). Krill oil-incorporated liposomes as an effective nanovehicle to ameliorate the inflammatory responses of DSS-induced colitis. *International Journal of Nanomedicine, 14*, 8305–8320. https://doi.org/10.2147/IJN.S220053

Kobayashi, T., Siegmund, B., Le Berre, C., Wei, S. C., Ferrante, M., Shen, B., … Hibi, T. (2020). Ulcerative colitis. *Nature Review Disorder Primers, 6*(74), 1–20. https://doi.org/10.1038/s41572-020-0205-x

Li, R. R., He, Q., Guo, M., Yuan, J. H., Wu, Y. Y., Wang, S. N., … Li, J. R. (2020a). Universal and simple method for facile fabrication of sustainable high internal phase emulsions solely using meat protein particles with various pH values. *Food Hydrocolloids, 100*, 1–10. https://doi.org/10.1016/j.foodhyd.2019.105444

Li, X. M., Li, X., Wu, Z., Wang, Y., Cheng, J. S., Wang, T., & Zhang, B. (2020b). Chitosan hydrochloride/carboxymethyl starch complex nanogels stabilized Pickering emulsions for oral delivery of beta-carotene: Protection effect and in vitro digestion study. *Food Chemistry, 315*, 1–9. https://doi.org/10.1016/j.foodchem.2020.126288

Liu, F., Smith, A. D., Solano-Aguilar, G., Wang, T. T. Y., Pham, Q., Beshah, E., … Li, R. W. (2020a). Mechanistic insights into the attenuation of intestinal inflammation and modulation of the gut microbiome by krill oil using in vitro and in vivo models. *Microbiome, 8*(83), 1–21. https://doi.org/10.1186/s40168-020-00843-8

Liu, K., Li, G., Guo, W., & Zhang, J. (2020b). The protective effect and mechanism of pedunculoside on DSS (dextran sulfate sodium) induced ulcerative colitis in mice. *International Immunopharmacology, 88*, 1–9. https://doi.org/10.1016/j.intimp.2020.107017

Liu, L., Bartke, N., Van Daele, H., Lawrence, P., Qin, X., Park, H. G., … Brenna, J. T. (2014). Higher efficacy of dietary DHA provided as a phospholipid than as a triglyceride for brain DHA accretion in neonatal piglets. *Journal of Lipid Research, 55*(3), 531–539. https://doi.org/10.1194/jlr.M045930

Liu, W., Gao, H., McClements, D. J., Zhou, L., Wu, J., & Zou, L. (2019). Stability, rheology, and β-carotene bioaccessibility of high internal phase emulsion gels. *Food Hydrocolloids, 88*, 210–217. https://doi.org/10.1016/j.foodhyd.2018.10.012

Liu, X., Guo, J., Wan, Z. L., Liu, Y. Y., Ruan, Q. J., & Yang, X. Q. (2018). Wheat gluten-stabilized high internal phase emulsions as mayonnaise replacers. *Food Hydrocolloids, 77*, 168–175. https://doi.org/10.1016/j.foodhyd.2017.09.032

Nikbakht Nasrabadi, M., Sedaghat Doost, A., Goli, S. A. H., & Van der Meeren, P. (2020). Effect of thymol and Pickering stabilization on in-vitro digestion fate and oxidation stability of plant-derived flaxseed oil emulsions. *Food Chemistry, 311*, Article 125872. https://doi.org/10.1016/j.foodchem.2019.125872

Pavan, E., Damazo, A. S., Arunachalam, K., Almeida, P. O. A., Oliveira, D. M., Venturini, C. L., … Martins, D. T. O. (2021). Copaifera malmei Harms leaves infusion attenuates TNBS-ulcerative colitis through modulation of cytokines, oxidative stress and mucus in experimental rats. *Journal of Ethnopharmacology, 267*, 1–9. https://doi.org/10.1016/j.jep.2020.113499

Piccolis, M., Bond, L. M., Kampmann, M., Pulimeno, P., Chitraju, C., Jayson, C. B. K., … Farese, R. V., Jr. (2019). Probing the global cellular responses to lipotoxicity caused by saturated fatty acids. *Molecular Cell, 74*(1), 32–44. https://doi.org/10.1016/j.molcel.2019.01.036

Qian, L., Li, J. Z., Sun, X., Chen, J. B., Dai, Y., Huang, Q. X., … Duan, Q. N. (2021). Safinamide prevents lipopolysaccharide (LPS)-induced inflammation in macrophages by suppressing TLR4/NF-kappaB signaling. *International Immunopharmacology, 96*, 1–7. https://doi.org/10.1016/j.intimp.2021.107712

Ren, Z., Li, Z., Chen, Z., Zhang, Y., Lin, X., Weng, W., … Li, B. (2021). Characteristics and application of fish oil-in-water pickering emulsions structured with tea water-insoluble proteins/κ-carrageenan complexes. *Food Hydrocolloids, 114*, 1–10. https://doi.org/10.1016/j.foodhyd.2020.106562

Sánchez, C. A. O., Zavaleta, E. B., García, G. R. U., Solano, G. L., & Díaz, M. P. R. (2021). Krill oil microencapsulation: Antioxidant activity, astaxanthin retention, encapsulation efficiency, fatty acids profile, in vitro bioaccessibility and storage stability. *LWT-Food Sci Technol, 147*, 1–10. https://doi.org/10.1016/j.lwt.2021.111476

Santos, T. P., Okuro, P. K., & Cunha, R. L. (2021). Pickering emulsions as a platform for structures design: Cutting-edge strategies to engineer digestibility. *Food Hydrocolloids, 116*, 1–10. https://doi.org/10.1016/j.foodhyd.2021.106645

Sharkawy, A., Barreiro, F., & Rodrigues, A. (2022). Pickering emulsions stabilized with chitosan/gum Arabic particles: Effect of chitosan degree of deacetylation on the physicochemical properties and cannabidiol (CBD) topical delivery. *Journal of Molecular Liquids, 355*. https://doi.org/10.1016/j.molliq.2022.118993

Sharkawy, A., Barreiro, M. F., & Rodrigues, A. E. (2019). Preparation of chitosan/gum Arabic nanoparticles and their use as novel stabilizers in oil/water Pickering emulsions. *Carbohydrate Polymers, 224*, Article 115190. https://doi.org/10.1016/j.carbpol.2019.115190

Sharkawy, A., Barreiro, M. F., & Rodrigues, A. E. (2020). Chitosan-based Pickering emulsions and their applications: A review. *Carbohydrate Polymers, 250*, Article 116885. https://doi.org/10.1016/j.carbpol.2020.116885

Sharkawy, A., Barreiro, M. F., & Rodrigues, A. E. (2021). New Pickering emulsions stabilized with chitosan/collagen peptides nanoparticles: Synthesis, characterization and tracking of the nanoparticles after skin application. *Colloids Surf Physicochem Eng Aspects, 616*. https://doi.org/10.1016/j.colsurfa.2021.126327

Sharkawy, A., Casimiro, F. M., Barreiro, M. F., & Rodrigues, A. E. (2020). Enhancing trans-resveratrol topical delivery and photostability through entrapment in chitosan/gum Arabic Pickering emulsions. *International Journal of Biological Macromolecules, 147*, 150–159. https://doi.org/10.1016/j.ijbiomac.2020.01.057

Sharkawy, A., Silva, A. M., Rodrigues, F., Barreiro, F., & Rodrigues, A. (2021). Pickering emulsions stabilized with chitosan/collagen peptides nanoparticles as green topical delivery vehicles for cannabidiol (CBD). *Colloids Surf Physicochem Eng Aspects, 631*. https://doi.org/10.1016/j.colsurfa.2021.127677

Taha, A., Hu, T., Zhang, Z., Bakry, A. M., Khalifa, I., Pan, S., & Hu, H. (2018). Effect of different oils and ultrasound emulsification conditions on the physicochemical properties of emulsions stabilized by soy protein isolate. *Ultrasonics Sonochemistry, 49*, 283–293. https://doi.org/10.1016/j.ultsonch.2018.08.020

Wei, Y., Tong, Z., Dai, L., Wang, D., Lv, P., Liu, J., … Gao, Y. (2020). Influence of interfacial compositions on the microstructure, physiochemical stability, lipid digestion and β-carotene bioaccessibility of Pickering emulsions. *Food Hydrocolloids, 104*, 1–16. https://doi.org/10.1016/j.foodhyd.2020.105738

Wei, Z. H., Cheng, Y. J., & Huang, Q. R. (2019). Heteroprotein complex formation of ovotransferrin and lysozyme: Fabrication of food-grade particles to stabilize Pickering emulsions. *Food Hydrocolloids, 96*, 190–200. https://doi.org/10.1016/j.foodhyd.2019.05.024

Wei, Z. H., Cheng, Y. J., Zhu, J. Y., & Huang, Q. R. (2019). Genipin-crosslinked ovotransferrin particle-stabilized Pickering emulsions as delivery vehicles for hesperidin. *Food Hydrocolloids, 94*, 561–573. https://doi.org/10.1016/j.foodhyd.2019.04.008

Wen, J., Zhang, Y., Jin, H., Sui, X., & Jiang, L. (2020). Deciphering the structural network that confers stability to high internal phase Pickering emulsions by cross-linked soy protein microgels and their in vitro digestion profiles. *Journal of Agriculture and Food Chemistry, 68*(36), 9796–9803. https://doi.org/10.1021/acs.jafc.0c03586

Wu, H. M., Wei, J., Wang, K., Qi, Y., & Wang, F. Y. (2018). Mucus protectors: Promising therapeutic strategies for inflammatory bowel disease. *Medical Hypotheses, 120*, 55–59. https://doi.org/10.1016/j.mehy.2018.08.013

Xiong, Q., Ru, Q., Tian, X., Zhou, M., Chen, L., Li, Y., & Li, C. (2018). Krill oil protects PC12 cells against methamphetamine-induced neurotoxicity by inhibiting apoptotic response and oxidative stress. *Nutrition Research, 58*, 84–94. https://doi.org/10.1016/j.nutres.2018.07.006

Yi, J., Gao, L., Zhong, G., & Fan, Y. (2020). Fabrication of high internal phase Pickering emulsions with calcium-crosslinked whey protein nanoparticles for beta-carotene stabilization and delivery. *Food & Function, 11*(1), 768–778. https://doi.org/10.1039/c9fo02434d

Zhang, M., Zhou, L., Yang, F., Yao, J., Ma, Y., & Liu, J. (2021). Construction of high internal phase Pickering emulsions stabilized by bamboo fungus protein gels with the effect of pH. *Food Chemistry, 369*, 1–6. https://doi.org/10.1016/j.foodchem.2021.130954

Zhou, F. Z., Huang, X. N., Wu, Z. L., Yin, S. W., Zhu, J. H., Tang, C. H., & Yang, X. Q. (2018). Fabrication of zein/pectin hybrid particle-stabilized Pickering high internal phase emulsions with robust and ordered interface architecture. *Journal of Agriculture and Food Chemistry, 66*(42), 11113–11123. https://doi.org/10.1021/acs.jafc.8b03714

Further reading

Abdullah, Weiss, J., Ahmad, T., Zhang, C., & Zhang, H. (2020). A review of recent progress on high internal-phase Pickering emulsions in food science. *Trends Food Science Technology, 106*, 91-103. http://doi.org/10.1016/j.tifs.2020.10.016.